The Mouse Model of Down Syndrome Ts65Dn Presents Visual Deficits as Assessed by Pattern Visual Evoked Potentials

Jonah Jacob Scott-McKean,[1] Bo Chang,[2] Ronald E. Hurd,[2] Steven Nusinowitz,[3] Cecilia Schmidt,[2] Muriel T. Davisson,[2] and Alberto C. S. Costa[1,4]

Purpose. The Ts65Dn mouse is the most complete widely available animal model of Down syndrome (DS). Quantitative information was generated about visual function in the Ts65Dn mouse by investigating their visual capabilities by means of electroretinography (ERG) and patterned visual evoked potentials (pVEPs).

Methods. pVEPs were recorded directly from specific regions of the binocular visual cortex of anesthetized mice in response to horizontal sinusoidal gratings of different spatial frequency, contrast, and luminance generated by a specialized video card and presented on a 21-in. computer display suitably linearized by gamma correction.

Results. ERG assessments indicated no significant deficit in retinal physiology in Ts65Dn mice compared with euploid control mice. The Ts65Dn mice were found to exhibit deficits in luminance threshold, spatial resolution, and contrast threshold, compared with the euploid control mice. The behavioral counterparts of these parameters are luminance sensitivity, visual acuity, and the inverse of contrast sensitivity, respectively.

Conclusions. DS includes various phenotypes associated with the visual system, including deficits in visual acuity, accommodation, and contrast sensitivity. The present study provides electrophysiological evidence of visual deficits in Ts65Dn mice that are similar to those reported in persons with DS. These findings strengthen the role of the Ts65Dn mouse as a model for DS. Also, given the historical assumption of integrity of the visual system in most behavioral assessments of Ts65Dn mice, such as the hidden-platform component of the Morris water maze, the visual deficits described herein may represent a significant confounding factor in the interpretation of results from such experiments. (*Invest Ophthalmol Vis Sci.* 2010;51: 3300–3308) DOI:10.1167/iovs.09-4465

Down syndrome (DS) is the most common genetically defined cause of intellectual disability and is produced by the trisomy of chromosome 21.[1] The approximate rate of live births with DS is 1 in 732 or 5429 each year, and the total estimated number of people with DS in the United States is roughly 300,000.[2] DS is typically accompanied by a moderate degree of intellectual disability, with an IQ range of 30 to 70.[3] In addition, individuals with DS have specific deficits in hippocampus-dependent and prefrontal cortex-dependent functions, affecting spatial learning, memory, and various aspects of language acquisition and comprehension.[4–7] DS is also associated with neuropathology, indistinguishable from that in Alzheimer's disease, that becomes universal by age 40.[8,9] Visual deficits similar to those in patients with Alzheimer disease also appear.[10]

Visual system impairments are an integral feature of DS and include deficits in visual acuity, accommodation, and contrast sensitivity.[11–18] Because a significant component of the visual deficits in persons with DS cannot be ameliorated through the use of corrective lenses, there is a strong possibility that a portion of such deficits are due to dysfunction of the central visual pathways.[17] This notion is supported by the finding of abnormal visual evoked potentials (VEPs) in adults[12,18] and children[15,17] with DS. Additional evidence of a neuronal origin of some visual deficits in persons with DS comes from the finding of altered dendritic and synaptic morphology in the cortex of individuals with DS.[19,20] Given the technical tools currently at our disposal, further advances in our understanding of the neurobiology of the visual deficits associated with DS would most certainly necessitate invasive approaches that would not be justifiable in human research settings.

In DS, as in many other fields of biomedical research, mouse models have proven to be essential tools for enhancing our understanding of the pathophysiology of clinical conditions and for testing new therapies in a preclinical setting. The Ts65Dn mouse is the most complete mouse model of DS that is widely available to the scientific community.[21,22] As a model of human trisomy 21, Ts65Dn mice display a remarkably diverse array of DS-like phenotypes, including performance deficits in different behavioral tasks and alterations in synaptic plasticity and adult neurogenesis.[23–34] Genetically, Ts65Dn mice are trisomic for the region of mouse chromosome 16 homologous to human chromosome 21, ranging from *Mrpl39* to *Znf295*,[35] which contains approximately 55% (i.e., 94/170) of the human chromosome 21 protein-coding gene mouse orthologues.[36]

From the [1]Neuroscience Training Program and the [4]Division of Clinical Pharmacology and Toxicology, Department of Medicine, University of Colorado School of Medicine, Aurora, Colorado; [2]The Jackson Laboratory, Bar Harbor, Maine; and the [3]Jules Stein Eye Institute, David Geffen School of Medicine, University of California, Los Angeles, California.

Supported by National Institute of Child Health and Human Development (NICHD) Contract HD73265 (MTD) and NICHD Grant HD056235 (ACSC). BC received support from National Eye Institute (NEI) Grant EY019943; ACSC received partial research support from the Anna and John J. Sie Foundation, the Coleman Institute for Cognitive Disabilities, Mile High Down Syndrome Association, and the Colorado Springs Down Syndrome Association.

Submitted for publication August 11, 2009; revised December 8, 2009, and January 12, 2010; accepted January 14, 2010.

Disclosure: **J.J. Scott-McKean**; None; **B. Chang**; None; **R.E. Hurd**, None; **S. Nusinowitz**, None; **C. Schmidt**, None; **M.T. Davisson**, None; **A.C.S. Costa**, None

Corresponding author: Alberto C. S. Costa, Division of Clinical Pharmacology and Toxicology, Department of Medicine, University of Colorado School of Medicine, 12700 East 19th Avenue, Campus Box C-237, Aurora, CO 80045; alberto.costa@ucdenver.edu.

The mouse visual system has been the focus of several studies in the quest for better understanding of how genetic mutations can affect vision. For example, different research teams have looked at mice lacking cone cells[37] and mice that display retinal degeneration.[38] Various groups have recorded VEPs and performed electroretinography (ERG) in mice. Most such VEP recordings, however, were obtained as flash VEPs, with the recording electrodes being placed on the scalp.[38–41] Pattern (p)VEPs are a powerful tool for detecting minor visual pathway abnormalities, are more sensitive than flash VEPs, and also have been performed in mice.[37,42–44] The use of pVEPs may provide a framework for characterizing visual phenotypes of a variety of transgenic and knockout mice and may complement behavioral experiments.

In the present study, we used ERG and VEP recordings to assess the functional integrity of the Ts65Dn retina and central visual system, respectively. Our ERG assessments indicated no significant deficit in retinal physiology in Ts65Dn mice compared to euploid control mice. However, we found that Ts65Dn mice display deficits in spatial resolution, contrast threshold, and luminance threshold when compared with littermate control mice. These results are qualitatively similar to those found in persons with DS and represent an important first step in the use of Ts65Dn mice as an experimental tool to help us understand how trisomy of the human chromosome 21 affects the visual system.

METHODS

Animals

The original production of the segmental trisomy Ts65Dn has been well described in the literature.[21,45] Experimental mice were generated by repeated backcrossing of Ts65Dn females to C57BL/6JEi × C3H/HeSnJ (B6EiC3H) F1 hybrid males in colonies in the Eleanor Roosevelt Institute at the University of Denver or The Jackson Laboratory (JAX). All mice were cytogenetically genotyped for the trisomic segment.[21] C3H/HeSnJ mice carry a recessive mutation that leads to retinal degeneration. Consequently, all animals were pre-evaluated by indirect ophthalmoscopy, and only mice without signs of retinal disease were used. The euploid littermates of Ts65Dn mice were used as control subjects. Up to five littermates of the same sex were housed in each cage and were maintained in a 12:12-hour light/dark schedule (lights on at 7 AM) with ad libitum access to food and water. Only males were tested in this study. The total number of mice per genotype used in the experiments was 25 Ts65Dn and 29 euploid control mice, aged 4 to 6 months. Only three Ts65Dn mice and three euploid control mice were used in both ERG and pVEP experiments (which were performed in two different institutions), all remaining animals were used only in a single modality of visual function assessment.

The animal procedures were approved by the Institutional Animal Care and Use Committees of the University of Denver, University of Colorado, and JAX and were conducted in accordance with the ARVO Statement for the Use of Animals in Ophthalmic and Vision Research. At the end of the experiments, all animals were killed by cervical dislocation and CO_2 asphyxiation without ever regaining consciousness from the urethane anesthesia.

Electroretinography

All ERG experiments were performed at JAX and by methods previously described by Nusinowitz et al.[44] and briefly described here. The mice were anesthetized with an intraperitoneal injection of xylazine (0.5 mg/mL) and ketamine (1 mg/mL) in normal saline. A volume of 6.25 mL/kg was administered. Body temperature was maintained at 37°C with a heating pad (Harvard Apparatus; Holliston, MA). Pupils were dilated with atropine (1%). For ERG recordings, a gold wire electrode was placed on the corneal surface of the right eye and referenced to a gold wire in the mouth. A needle electrode in the tail served as the ground. The left eye (not stimulated) was occluded with a dark patch during the ERG recordings. Responses were amplified (CP511 AC Amplifier, ×10,000; Grass Instruments, Warwick, RI), band-pass filtered (1–300 Hz), digitized with an I/O board (Laboratory-PC-1200; National Instruments, Austin, TX) into a personal computer, and averaged. After overnight dark adaptation of the mice, rod-mediated responses were recorded to short-wavelength (λ_{max} = 470 nm; Wratten 47A filter; Eastman Kodak, Rochester, NY), flashed stimuli over a 4.0-log-unit range of intensities. Flash intensity was varied in 0.3-log-unit intervals by combinations of neutral-density filters and intensity settings on the photostimulator control unit. Flash-presentation frequency was 1 Hz, except at the highest intensities, in which the presentation rate was 0.2 Hz. Cone-mediated responses were obtained with white flashes on a rod-saturating background (32 cd/m^2) and after 10 minutes of light adaptation.[37]

Surgery

All pVEP experiments were conducted at the University of Denver. Mice were anesthetized with 20% urethane (Sigma-Aldrich, St. Louis, MO) in PBS by intraperitoneal injection (6.25 mL/kg). A portion of the skull was removed with a dental drill (Handpiece Specialists, Inc., Welches, OR), leaving the dura intact. Mineral oil was placed on the exposed cortex to reduce loss of moisture. A few drops of a commercial eye preparation of 0.5% carboxymethylcellulose sodium was instilled onto both eyes to keep the cornea moist and to prevent the formation of cataracts.[46] At the end of the experiments, the eyes were checked for cataracts by indirect ophthalmoscopy.

Apparatus

The mice were placed in a small-animal stereotaxic system (EM70G; David Kopf Instruments, Tujunga, CA) that was modified to allow a full view of the visual stimulus. Body temperature was monitored and maintained at 37°C with the aid of a rectal temperature probe and a heating pad (Harvard Apparatus). A pulse oximeter (CANL-425SV-A; Med Associates, St. Albans, VT) was attached to the tail vein to measure the oxygen saturation and pulse rate of the animals during the experiments and assure that the percentage of arterial hemoglobin in the oxyhemoglobin configuration was maintained at a minimum of 85% during the entire course of the experiment. To obtain an 81° × 86° visual field, we placed the computer screen 16.78 cm from the mouse and centered it on the midpoint of the line segment between the middle of the animal's eyes.

Visual Stimuli

Visual stimuli consisted of horizontal sinusoidal gratings of different spatial frequencies (0.04, 0.06, 0.08, 0.12, 0.16, 0.20, 0.24, 0.30, 0.40, and 0.48 cyc/deg), contrast (100%, 90%, 80%, 70%, 60%, 50%, 40%, 30%, 20%, 15%, 10%, 7.5%, and 5%), and luminance (30, 15, 7.5, 3.75, 1.87, 0.94, and 0.47 cd/m^2), generated by a specialized video card (Cambridge Research System, Rochester, UK) and presented on a 21-in. computer display (1024 × 768 at 120 Hz; FD Trinitron; Sony, Tokyo, Japan) suitably linearized by gamma correction. Transient VEPs were induced by the stepwise reversal of the spatial contrast (i.e., by a 180° phase shift) of sinusoidal gratings at 1 Hz. Stimulus contrast (Michelson contrast) is expressed in percentage, as $c = 100(L_{max} - L_{min})/(L_{max} + L_{min})$, where L_{max} and L_{min} are maximum and minimum luminances, respectively.

Electrophysiological Recording of pVEPs

A glass-coated metal (platinum 80%/iridium 20%) electrode (FHC, Bowdoinham, ME), with a tip impedance of 0.5 MΩ, was inserted into the visual cortex 3.0 mm lateral to lambda,[42] to detect ensemble VEPs. Except for the laminar analysis experiments, the electrode was advanced 400 μm to record from layer IV of the primary visual cortex. In experiments involving laminar analysis, microelectrodes were advanced 50 to 800 μm in 50-μm steps within the cortex, and the

electrode track was reconstructed by electrolytic lesions (5 mA, 5 seconds) made at different cortical depths. The electrode was advanced with a three-axis electrode micromanipulator with a digital display and a resolution of 1 μm (EM70G; David Kopf Instruments). The resulting signals were then amplified by an AC differential amplifier ($\times$1000, DAM 80; World Precision Instruments, Sarasota, FL) and then passed through a 50/60 cycle noise eliminator (Hum Bug; Quest Scientific, North Vancouver, BC, Canada). The signal was then amplified another 20-fold by an instrumentation amplifier (Precision Electrophysiology Amplifier with signal conditioner Model 440; Brownlee San Jose, CA), band-pass filtered (0.1–100 Hz, −3 dB), and digitized (16-bit resolution) into a computer at a sampling rate of 1 kHz (Digidata 1322A; Axon Instruments, Union City, CA). Data acquisition, online averaging (at least 100 events synchronized to the stimulus contrast reversal), and off-line analysis of data were performed with allied software (pCLAMP; Axon Instruments).

Data Analysis

Data are expressed as the mean and SEM. VEP peak amplitudes were measured from peak to baseline and only signals that had amplitudes at least two standard deviations above the baseline noise were included in the data analysis. Luminance dependence of the pVEP peak amplitude and peak delay were assessed by subjecting the mice to stimuli of progressively lower luminance, and mean peak amplitude of pVEPs recorded from each mouse were averaged and plotted on a logarithmic scale. Spatial resolution and contrast threshold for each genotype were determined by the linear extrapolation to the 0-μV amplitude of the regression line between the individual pVEP amplitudes and the respective stimulus contrasts and spatial frequencies (plotted on a semilogarithmic scale). At least four data points in the lower amplitude range (i.e., the shallow-slope linear range of the graph) were used in linear extrapolation analyses This method was adapted from the study by Campbell and Maffei.[47] In their classic work, the authors found that the semilogarithmic graphing of pVEP amplitudes and the use of the 0-μV amplitude extrapolation procedure for lower pVEP amplitudes produces measures that correspond closely to psychophysical thresholds. Spatial resolution and contrast threshold were analyzed by two-tailed, unpaired *t*-tests with Welch's correction (Prism ver. 5; GraphPad Software, San Diego, CA). All other data were analyzed by two-way, repeated-measures analysis of variance (RM ANOVA), and post hoc multiple comparisons were performed by the Fisher protected least significant difference (PLSD) test (Statistica 7.0; Stat-soft, Tulsa, OK). In the figures, statistical significance is expressed as $^{*}P < 0.05$, $^{**}P < 0.01$, and $^{***}P < 0.001$.

Results

Electroretinography

To investigate the presence of potential differences in retinal physiology between Ts65Dn and euploid control mice, we assessed quantitatively ERG responses to flash stimuli of various intensities. A dark-adapted ERG protocol was used to test rod-mediated function (representative traces shown in Figs. 1A, 1B) and a light-adapted protocol was use to test cone-mediated function (representative traces shown in Figs. 1C, 1D). Peak means were averaged and plotted on a logarithmic scale (Figs. 1E, 1F). For the dark-adapted protocol, two-way RM ANOVA revealed a significant stimulus-intensity dependence ($F_{10,140} = 242.34$, $P < 0.001$), but no significant genotype dependence ($F_{1,14} = 0.37$, $P = 0.55$) for the ERG peak amplitude. In addition, we found no significant interaction between stimulus intensity and genotype for the results obtained in the dark-adapted protocol ($F_{10,140} = 1.43$; $P = 0.17$). In contrast, analysis of data obtained using the light-adapted protocol showed neither stimulus-intensity dependence ($F_{4,76} = 0.71$, $P = 0.59$) nor genotype dependence ($F_{1,19} = 2.69$, $P = 0.12$) for the ERG peak amplitude. Finally, similar to the results obtained in the dark-adapted protocol, we did not detect any significant interaction between stimulus intensity and genotype for the results obtained in the light-adapted protocol ($F_{4,76} = 0.73$; $P = 0.57$).

Laminar Analysis

To determine the proper depth for recording robust pVEPs, we placed the electrode at various depths (varying from 50–800 μm, in 50-μm increments) in the primary visual cortex of both the Ts65Dn and the euploid littermate control mice. VEPs were induced by a full-field reversing stimulus consisting of horizontal sinusoidal gratings of 90% contrast and 0.06-cyc/deg spatial frequency, which was reversed in a stepwise fashion at 1 Hz. As was previously reported,[42] the pVEP waveforms were very simple, with a major component peaking at 90 to 100 ms. In superficial layers (50–250-μm electrode advancement) the waveform was positive. In deeper layers, however, the waveform was negative. Figures 2A and 2B show traces resulting from the advance of the electrode deeper into the visual cortex. The intracortical pVEP profiles showed clear polarity inversion between 250 and 300 μm for both genotypes. Also in agreement with previous work, a depth of 400 μm was determined to be optimal for recording maximum-amplitude, negative-peak pVEPs in the euploid control mice, which was true for the Ts65Dn mice as well (Fig. 2C). These findings suggest that the VEP in the Ts65Dn and control mice are generated at the same laminar location in the visual cortex.

It should be noted that the particular traces depicted in Figure 2 can be considered somewhat atypical for this study, because the pVEP peak amplitudes recorded from Ts65Dn mice were generally larger than those from control mice. In experiments in which mean values were obtained from a fairly large number of animals (see Figs 3, 4, 5), the mean pVEP peak amplitudes recorded from the Ts65Dn mice were consistently lower than those recorded in the control mice. It should be noted, however, that these data are well within the observed individual variability in each genotype group.

Luminance Dependence

Whether there was genotype and/or stimulus luminance dependence of the pVEP peak amplitude and peak delay was determined by subjecting the mice to stimuli of progressively lower luminance. In general, decreasing the stimulus luminance (in candelas per square meter) resulted in decreased pVEP amplitudes (Figs. 3A, 3B) and increased pVEP latencies (Fig. 3C). Responses measurably larger than the baseline noise were recorded throughout the test in all the control animals. However, pVEPs recorded from the Ts65Dn mice had smaller average amplitude than those from the euploid control mice. Consequently, pVEPs from many of the Ts65Dn mice were not detectable at the lowest stimulus luminance (i.e., the Ts65Dn mice had a higher luminance threshold than the euploid mice had). In accordance with these observed qualitative differences, two-way RM-ANOVA showed significant luminance ($F_{6,132} = 16.43$, $P < 0.001$) and genotype ($F_{1,22} = 9.73$, $P = 0.005$) dependence for pVEP amplitude, and a significant interaction between stimulus luminance and mouse genotype ($F_{6,132} = 2.53$, $P = 0.024$). In addition, post hoc analysis revealed that, irrespective of the stimulus luminance, Ts65Dn mice displayed smaller pVEP amplitudes than did euploid control mice ($P < 0.001$, for all stimulus luminances).

We also detected a significant luminance dependence for peak latency ($F_{6,120} = 7.89$, $P < 0.001$) and a significant interaction between stimulus luminance and mouse genotype for peak latency ($F_{6,120} = 2.43$, $P = 0.030$). However, we found no significant genotype dependence for peak latency ($F_{1,20} = 0.0024$, $P = 0.96$).

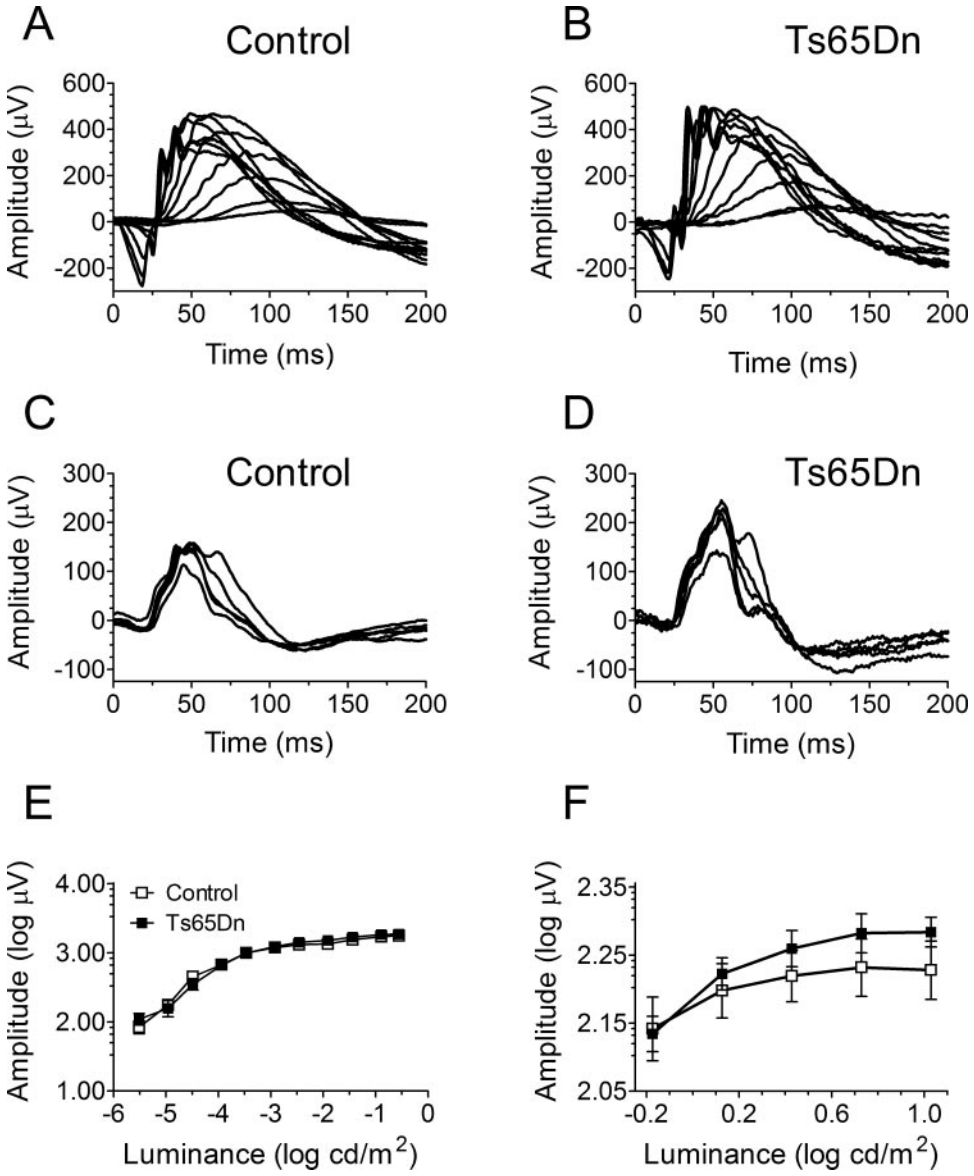

FIGURE 1. ERG recordings in dark- and light-adapted protocols. Representative traces from control and Ts65Dn mice, respectively, in the (**A**, **B**) dark-adapted and (**C**, **D**) light-adapted protocols. Mean ERG ± SEM peak amplitudes for euploid control ($n = 9$) and Ts65Dn ($n = 9$) mice under the (**E**) dark-adapted protocol (note that error bars are smaller than symbols in this figure) and (**F**) light-adapted protocols.

Spatial Resolution

We determined whether spatial resolution was dependent on genotype by subjecting the mice to stimuli of progressively higher spatial frequencies. In general, the pVEP amplitude was inversely proportional to the stimulus spatial frequency, with mean pVEP amplitudes in the Ts65Dn mice being smaller than those of the control euploid mice (Fig. 4A). Accordingly, two-way RM-ANOVA revealed a significant spatial frequency ($F_{9,198} = 32.92$, $P < 0.001$) and genotype ($F_{1,22} = 5.14$, $P = 0.034$) dependence of the pVEP amplitude. Nevertheless, no interaction was found between stimulus and mouse genotype ($F_{9,198} = 1.78$, $P = 0.073$). Fisher's PLSD post hoc tests detected significant genotype-dependent differences for the following stimulus spatial frequencies: 0.04 ($P < 0.001$), 0.06 ($P = 0.0019$), 0.08 ($P = 0.016$), 0.12 ($P < 0.001$), and 0.16 ($P = 0.0016$) cyc/deg. (Note that responses measurably larger than the baseline noise were recorded routinely at spatial frequencies higher than 0.4 cyc/deg in the control animals, whereas it was unusual for us to detect any response from the Ts65Dn mice at this spatial frequency and higher.)

Spatial resolution, which is the electrophysiological correlate of visual acuity, was determined by linearly extrapolating to the 0-μV amplitude the regression line between the individual pVEP amplitudes and the corresponding stimulus spatial frequencies (plotted on a semilogarithmic scale)[42,47,48] (Figs. 4B, 4C). We found that the spatial resolution calculated by this method was significantly lower in the Ts65Dn mice (0.29 ± 0.038 cyc/deg; $n = 12$) compared with that in the control euploid mice (0.47 ± 0.043 cyc/deg; n = 12; $P = 0.0066$; unpaired *t*-test with Welch's correction; Fig. 4D).

Contrast Threshold

To determine whether contrast threshold was dependent on genotype, we subjected the mice to stimuli of progressively lower contrast. The percentage of contrast represents the peak-to-valley difference in pixels for the sinusoidal gratings

(with black versus white being defined as 100% contrast). As illustrated in Figure 5A, the pVEP amplitude was directly proportional to the stimulus contrast. Two-way RM-ANOVA confirmed this dependence of the pVEP amplitude on the stimulus contrast threshold ($F_{11,242} = 70.99$, $P < 0.001$). The pVEP amplitude, however, was not significantly genotype dependent ($F_{1,22} = 3.75$, $P = 0.066$). Furthermore, no significant interaction between stimulus contrast and mouse genotype was detected ($F_{11,242} = 1.17$, $P = 0.31$).

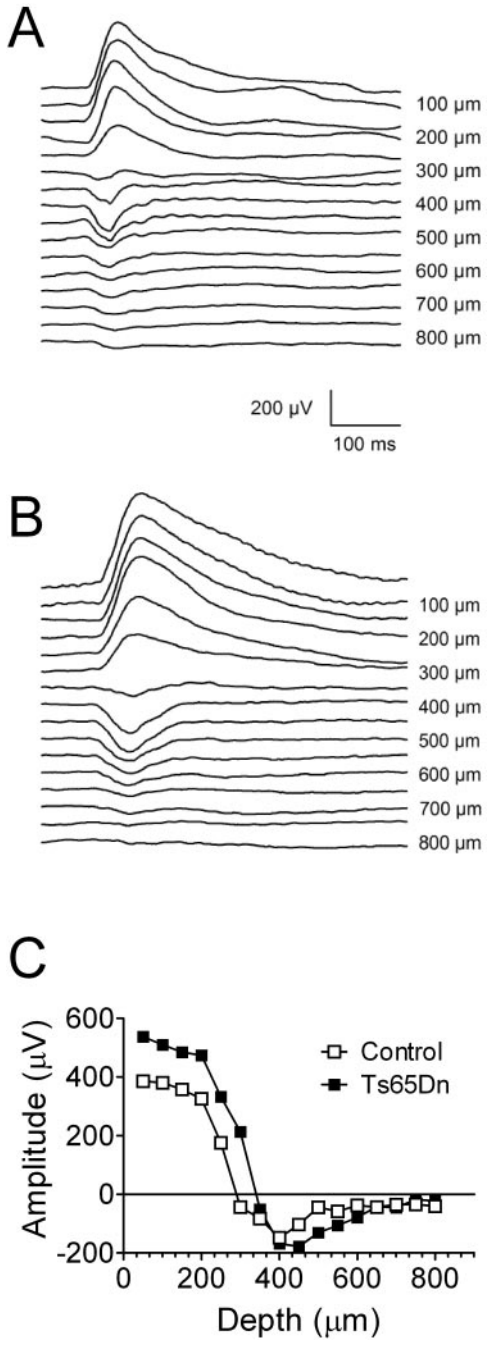

FIGURE 2. VEP recordings at different electrode penetration depths (for laminar analysis) from the primary visual cortex in Ts65Dn and euploid control mice. The mice were stimulated with 1-Hz reversing full-field gratings (90% contrast, 30 cd/m^2 luminance, 0.06 cyc/deg spatial frequency). pVEP recordings from (**A**) a euploid control mouse and (**B**) a Ts65Dn mouse. (**C**) Summary of laminar analysis showing an optimal recording depth of 400 μm for both euploid control and Ts65Dn mice.

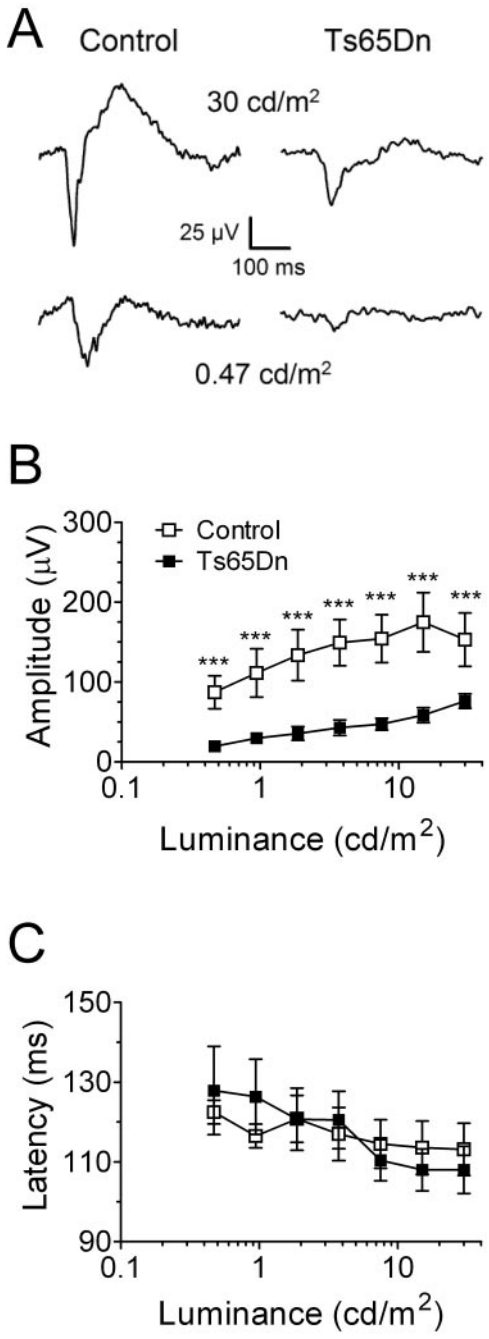

FIGURE 3. Stimulus luminance × VEP amplitude and stimulus luminance × pVEP peak latency relationships for Ts65Dn and euploid control mice. (**A**) Representative pVEP traces produced by two different stimulus luminances (30 and 0.47 cd/m^2) obtained from control (*left*) and Ts65Dn (*right*) mice. Stimulus luminance × pVEP (**B**) mean amplitude and (**C**) mean peak latency. ***$P < 0.001$.

We found that, typically, responses measurably larger than the baseline noise were recorded at stimulus contrasts up to 5% in the euploid control mice, but it was unusual for Ts65Dn mice to display responses to this low level of contrast. To determine contrast thresholds, we again used the method of linearly extrapolating to the 0-μV amplitude the regression line between the individual pVEP amplitudes and the corresponding stimulus contrasts (plotted on a semi-logarithmic

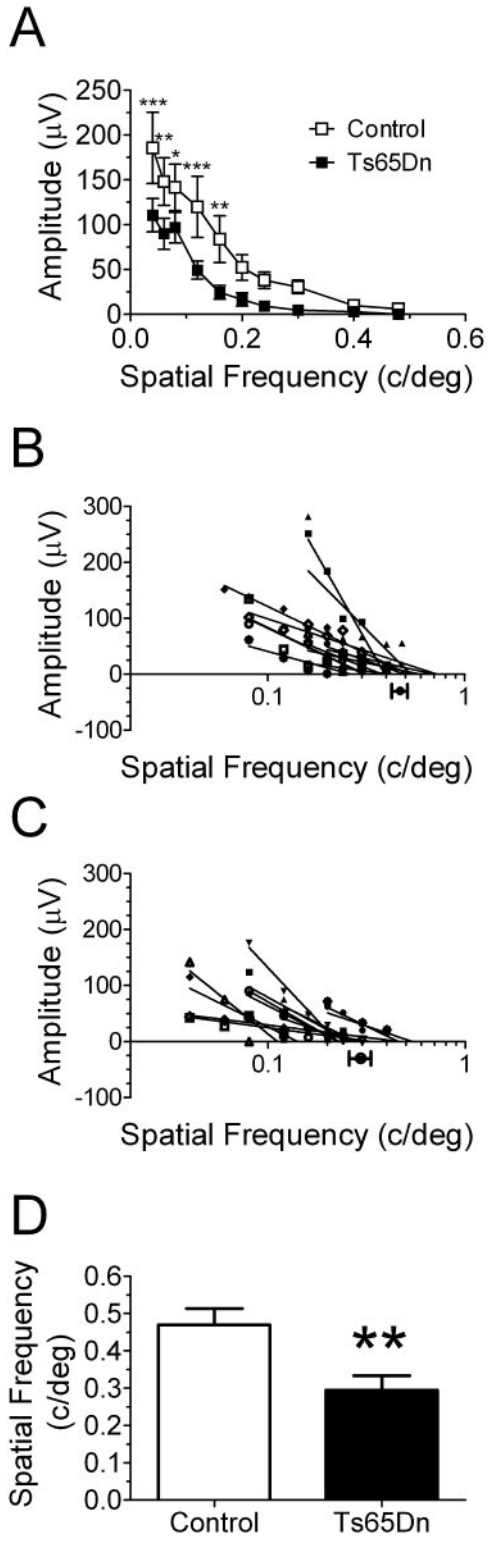

FIGURE 4. Spatial resolution assessments for Ts65Dn and euploid control mice. (**A**) Mean pVEP amplitudes for euploid control and Ts65Dn mice. Spatial resolutions were determined by linear extrapolation to 0 V for pVEP peak amplitudes in response to stimuli of progressively higher spatial frequency (plotted on a semilogarithmic scale) recorded from each control (**B**) and Ts65Dn (**C**) mouse. (**B**, **C**) *Filled circles* and *horizontal bars* below the *x*-axis: mean spatial resolution ± SEM for control ($n = 12$) and Ts65Dn ($n = 12$) mice. (**D**) Direct comparison of mean spatial resolution ± SEM for euploid control (□) and Ts65Dn (■) mice, which were abstracted from the linear extrapolations of the individual VEP amplitudes to the 0-μV line depicted in (**B**) and (**C**). $^{*}P < 0.05$; $^{**}P < 0.01$; $^{***}P < 0.001$.

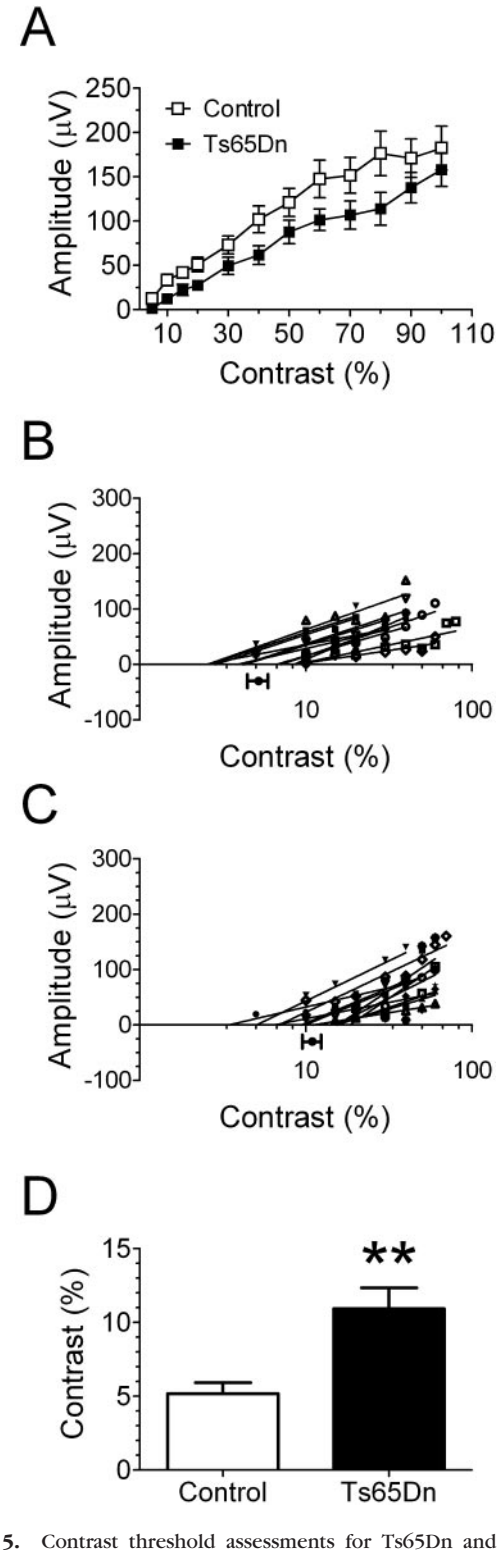

FIGURE 5. Contrast threshold assessments for Ts65Dn and euploid control mice. (**A**) Mean pVEP amplitude ± SEM for euploid control and Ts65Dn mice. Contrast thresholds were determined by linear extrapolation to 0 V for pVEP peak amplitudes in response to stimuli of progressively lower contrasts (plotted on a semilogarithmic scale) recorded from each control (**B**) and Ts65Dn (**C**) mouse. (**B**, **C**) *Filled circles* and *horizontal bars* below the *x*-axis in (**B**) and (**C**) represent the mean contrast threshold ± SEM for control ($n = 12$) and Ts65Dn ($n = 12$) mice. (**D**) Direct comparison of mean of contrast threshold ± SEM for euploid control (□) and Ts65Dn (■) mice, which were abstracted from the linear extrapolations of the individual VEP amplitudes to the 0-μV line depicted in (**B**) and (**C**). $^{**}P < 0.01$.

scale)[42,47,48] (Figs. 5B, 5C). Statistical comparison of the mean contrast thresholds between values obtained revealed a reduced contrast threshold ($P = 0.0023$; unpaired *t*-test with Welch's correction) in the Ts65Dn mice (10.94% ± 1.41%; $n = 12$) compared with that in the euploid control mice (5.18% ± 0.73%; $n = 12$; Fig. 5D).

Discussion

The Ts65Dn mouse continues to gain prominence in the field of DS research as the most complete mouse model for DS that is widely available. Over the past two decades, results from several laboratories have unveiled many DS-like phenotypes in these mice.[31–34] In this study, we continued the historical trend by presenting results supporting the hypothesis that the Ts65Dn trisomic segment is sufficient to produce many DS-like visual deficits. For example, similar to persons with DS, the Ts65Dn mice produced pVEPs of significantly smaller amplitudes than littermate control mice in response to all stimulus luminances tested. The Ts65Dn mice had lower spatial resolution (the electrophysiological correlate of visual acuity) and higher contrast threshold (the electrophysiological inverse correlate of contrast sensitivity) than did the euploid control mice. These findings are relevant to the modeling of DS, because individuals with DS display decreased visual acuity and reduced contrast sensitivity when compared with the general population. It is noteworthy that, although the observed genotype effects were small (≈0.45 cyc/deg vs. ≈0.30 cyc/deg for spatial resolution, and ≈5% vs. ≈10% for contrast threshold), these reductions are of a magnitude similar to those reported in persons with DS,[17] which provides further evidence to support the Ts65Dn mouse as a model of DS. In addition, because the VEPs in the present study were recorded from mice (which have nonfoveate retinas) under anesthesia, the effects of attention and fixation should have been negligible. Therefore, our results also help strengthen previous assessments in persons with DS, which have the inherent potential confounder of defocusing and of distracted attention, both of which can produce false-positive results (reduced VEP with prolonged time-to-peak) in young subjects when small checks are used as pVEP stimuli.[49]

In this study, we did not observe an increase in pVEP latency in the Ts65Dn mice similar to that typically seen in persons with DS. Yet, it is possible that this discrepancy between pVEP findings in Ts65Dn mice and persons with DS may simply be the result of the considerable physical difference in the length of the optical pathways in mice and human beings—the argument being that, in the short pathway the visual stimulus has to travel in the mouse brain, differences and electrical conduction speed, due for example to differences in axonal diameter or myelination, should have less of an effect than on the much longer human visual pathway. For example, recent work by Martin et al.[50] has shown very small VEP delays (≈2 ms) in shiverer heterozygous (*Mbp*^{sbi}/+) mutant mice, even though these animals display severe hypomyelination of the optic nerve and the optic tract. In contrast, VEP latency has been used as a reliable indicator of the severity of demyelination of the central nervous system in persons with multiple sclerosis[51] (with typical VEP delays being 15 to 20 ms), although in many instances, the level of demyelination in such patients is comparatively milder than that observed in *Mbp*^{sbi}/+ mutant mice.

Although pVEPs have been used to assess visual function in mutant mice,[37,38,50,52,53] there has been no report of the use of this technique in a mouse model of a human brain disorder. Although flash VEPs have been recorded in amyloid precursor protein transgenic mice,[53] those investigators did not use pVEPs, which means that they could not assess spatial resolution or contrast threshold in the mice. In addition, it is unlikely that the small, but significant differences observed in contrast threshold and spatial resolution between the genotypes reported herein could have been detected reliably with the use of scalp electrodes. Therefore, the findings from the present study should establish an important precedent for the use of pVEPs for the study of animal models of human neurologic and neuropsychiatric diseases that produce deficits in visual parameters as seen, for example, with the visual deficits reported in Alzheimer disease.[54–56]

The present study was not meant to be a comprehensive investigation of the visual physiology of Ts65Dn mice, but rather, a first approach to this area of inquiry. Our primary goals were to validate further the use of these animals as a mouse model of DS and to raise awareness of potential confounders in the interpretation of some behavioral assessments in Ts65Dn mice. We believe we accomplished these goals in the present study. Nevertheless, we are also aware that we have not addressed other ophthalmic and neuroophthalmic disorders frequently seen in persons with DS, such as strabismus, spontaneous and latent nystagmi, deficiencies in accommodation, and refractive errors, which may also be phenotypes of the Ts65Dn mouse and may help explain some of our findings. It is important to point out, however, that in a published human VEP study,[12] even subjects with DS who did not present any of these ophthalmic and neuroophthalmic disorders showed significant reductions in VEP amplitude compared with typical control individuals. In addition, altered dendrite arbors and dendritic spine morphology have been described in brain specimens from persons with DS and from Ts65Dn mice,[19,20] which provide some support to a potential neural sensory origin to the pVEP phenotypes we observed in the Ts65Dn mice. Finally, our coarse comparative laminar analysis of the visual cortex of control and Ts65Dn mice showed no differences in terms of the depth at which the pVEP peak polarity reversals occur (i.e., between 250 and 300 μm) or the depth at which the maximum negative pVEP peaks could be recorded (400 μm). Given that these results agree with historical data,[42] we have not proceeded to record data from a sufficient number of animals to perform meaningful statistical analyses. Because of the high quality of our stereotactic apparatus and the extreme care taken during the execution of the electrophysiological recordings described herein, it is improbable that the depth of electrode placement varied by more than a few micrometers from animal to animal. However, because the diameters of our electrolytic lesions were as large as 50 μm, they were not precise enough to discriminate histologically small electrode depth differences that could have had a potentially significant impact on VEP amplitudes. Also, in the present study, we did not attempt to perform a quantitative analysis of the thickness of the layers of the visual cortex of the Ts65Dn versus the euploid control mice. This comparison is of importance because even a fairly subtle level of cortical dysmorphology in Ts65Dn mice could contribute to the genotype effect on pVEP amplitudes observed in the present study. Therefore, more work involving finer electrode advancements/electrolytic marking and careful histologic analysis is needed to determine whether significant dysmorphology is present in the cortical layers of Ts65Dn mice compared with those of euploid control animals. However, it is also important to note that the linear extrapolation analysis used for the determination of the two most clinically relevant phenotypes assessed in this study (i.e., spatial resolution and contrast threshold), should not be affected significantly by animal-to-animal variations in VEP amplitudes.

The present results may also further assist the identification of potential confounders to the interpretation of behavioral

studies using Ts65Dn mice and other animal models of DS; particularly those involving the Morris water maze. In the field of DS research, the Morris water maze has been used extensively in the search for potential surrogate markers of DS-like hippocampus dysfunction in the Ts65Dn mouse since 1995.[57–61] The performance on the hidden platform component of the task is impaired by hippocampal lesion in both rats[62] and mice.[63] However, different laboratories use different types of extramaze cues. Often, such cues are simply room landmarks, such as doors, laboratory furniture, and laboratory equipment. Therefore, depending on the level of contrast of the extramaze cues (e.g., gray cabinets in an experimental room with gray painted laboratory walls), even mild-to-moderate visual deficits (such as those of Ts65Dn versus control euploid mice, as predicted from the analysis of the pVEP data presented herein) have the potential to reduce significantly an animal's ability to use such landmarks for navigation. These potential confounders can become particularly problematic in the interpretation of Morris water maze data when the difference in performance between experimental and control rodents is small, which is exactly the case with Ts65Dn mice.[59] Unfortunately, the standard Morris water maze visual control, the visible platform task is too crude to identify the potential behavioral effects of mild-to-moderate visual deficits. As noted by Robinson et al.,[64] even animals with severe visual deficits may be perfectly able to solve this task, as the cued platform stands out from the surrounding environment. Consequently, even with the use of the cued platform control experiment, in which the Ts65Dn mouse typically performs at the same level as the euploid control, visual deficits can still represent a significant confounding factor in the interpretation of the results of Morris water maze experiments.

Finally, a better understanding of the visual system of individuals with DS through the use of mouse models could eventually lead to more targeted pharmacologic and rehabilitative therapies and improved educational opportunities and quality of life for persons with DS.

References

1. Lejeune J. Le mongolism: premier exemple d'aberration autosomique humaine. *Ann Genet.* 1959;1:1–49.
2. Canfield MA, Honein MA, Yuskiv N, et al. National estimates and race/ethnic-specific variation of selected birth defects in the United States 1999–2001. *Birth Defects Res A Clin Mol Teratol.* 2006;76:747–756.
3. Turner S, Alborz A. Academic attainments of children with Down's syndrome: a longitudinal study. *Br J Educ Psychol.* 2003;73:563–583.
4. Abbeduto L, Warren SF, Conners FA. Language development in Down syndrome: from the prelinguistic period to the acquisition of literacy. *Ment Retard Dev Disabil Res Rev.* 2007;13:247–261.
5. Pennington BF, Moon J, Edgin J, Stedron J, Nadel L. The neuropsychology of Down syndrome: evidence for hippocampal dysfunction. *Child Dev.* 2003;74:75–93.
6. Chapman RS. Language learning in Down syndrome: the speech and language profile compared to adolescents with cognitive impairment of unknown origin. *Downs Syndr Res Pract.* 2006;10:61–66.
7. Chapman RS, Hesketh LJ. Behavioral phenotype of individuals with Down syndrome. *Ment Retard Dev Disabil Res Rev.* 2000;6:84–95.
8. Wisniewski KE, Dalton AJ, McLachlan C, Wen GY, Wisniewski HM. Alzheimer's disease in Down's syndrome: clinicopathologic studies. *Neurology.* 1985;35:957–961.
9. Iwatsubo T, Mann DM, Odaka A, Suzuki N, Ihara Y. Amyloid beta protein (A beta) deposition: A beta 42(43) precedes A beta 40 in Down syndrome. *Ann Neurol.* 1995;37:294–299.
10. Rocco FJ, Cronin-Golomb A, Lai F. Alzheimer-like visual deficits in Down syndrome. *Alzheimer Dis Assoc Disord.* 1997;11:88–98.
11. Courage ML, Adams RJ, Reyno S, Kwa PG. Visual acuity in infants and children with Down syndrome. *Dev Med Child Neurol.* 1994;36:586–593.
12. Kakigi R, Oono S, Matsuda Y, Kuroda Y. Pattern-reversal visual evoked potentials in Down's syndrome. *Acta Neurol Scand.* 1993;87:410–415.
13. Perez-Carpinell J, de Fez MD, Climent V. Vision evaluation in people with Down's syndrome. *Ophthalmic Physiol Opt.* 1994;14:115–121.
14. Gardiner PA. Visual defects in cases of Down's syndrome and in other mentally handicapped children. *Br J Ophthalmol.* 1967;51:469–474.
15. Suttle CM, Turner AM. Transient pattern visual evoked potentials in children with Down's syndrome. *Ophthalmic Physiol Opt.* 2004;24:91–99.
16. Woodhouse JM, Cregg M, Gunter HL, et al. The effect of age, size of target, and cognitive factors on accommodative responses of children with Down syndrome. *Invest Ophthalmol Vis Sci.* 2000;41:2479–2485.
17. John FM, Bromham NR, Woodhouse JM, Candy TR. Spatial vision deficits in infants and children with Down syndrome. *Invest Ophthalmol Vis Sci.* 2004;45:1566–1572.
18. Suttle CM, Lloyd R. Chromatic and achromatic transient VEPs in adults with Down syndrome. *Ophthalmic Physiol Opt.* 2005;25:501–513.
19. Becker L, Mito T, Takashima S, Onodera K. Growth and development of the brain in Down syndrome. *Prog Clin Biol Res.* 1991;373:133–152.
20. Benavides-Piccione R, Ballesteros-Yanez I, de Lagran MM, et al. On dendrites in Down syndrome and DS murine models: a spiny way to learn. *Prog Neurobiol.* 2004;74:111–126.
21. Davisson MT, Schmidt C, Reeves RH, et al. Segmental trisomy as a mouse model for Down syndrome. *Prog Clin Biol Res.* 1993;384:117–133.
22. Reeves RH, Irving NG, Moran TH, et al. A mouse model for Down syndrome exhibits learning and behaviour deficits. *Nat Genet.* 1995;11:177–184.
23. Costa AC, Grybko MJ. Deficits in hippocampal CA1 LTP induced by TBS but not HFS in the Ts65Dn mouse: a model of Down syndrome. *Neurosci Lett.* 2005;382:317–322.
24. Costa AC, Scott-McKean JJ, Stasko MR. Acute injections of the NMDA receptor antagonist memantine rescue performance deficits of the Ts65Dn mouse model of Down syndrome on a fear conditioning test. *Neuropsychopharmacology.* 2008;33:1624–1632.
25. Demas GE, Nelson RJ, Krueger BK, Yarowsky PJ. Spatial memory deficits in segmental trisomic Ts65Dn mice. *Behav Brain Res.* 1996;82:85–92.
26. Demas GE, Nelson RJ, Krueger BK, Yarowsky PJ. Impaired spatial working and reference memory in segmental trisomy (Ts65Dn) mice. *Behav Brain Res.* 1998;90:199–201.
27. Dowdy-Sanders NC, Wenger GR. Working memory in the Ts65Dn mouse, a model for Down syndrome. *Behav Brain Res.* 2006;168:349–352.
28. Siarey RJ, Carlson EJ, Epstein CJ, Balbo A, Rapoport SI, Galdzicki Z. Increased synaptic depression in the Ts65Dn mouse, a model for mental retardation in Down syndrome. *Neuropharmacology.* 1999;38:1917–1920.
29. Siarey RJ, Stoll J, Rapoport SI, Galdzicki Z. Altered long-term potentiation in the young and old Ts65Dn mouse, a model for Down syndrome. *Neuropharmacology.* 1997;36:1549–1554.
30. Clark S, Schwalbe J, Stasko MR, Yarowsky PJ, Costa AC. Fluoxetine rescues deficient neurogenesis in hippocampus of the Ts65Dn mouse model for Down syndrome. *Exp Neurol.* 2006;200:256–261.
31. Patterson D, Costa AC. Down syndrome and genetics: a case of linked histories. *Nat Rev Genet.* 2005;6:137–147.
32. Belichenko PV, Masliah E, Kleschevnikov AM, et al. Synaptic structural abnormalities in the Ts65Dn mouse model of Down Syndrome. *J Comp Neurol.* 2004;480:281–298.
33. Richtsmeier JT, Zumwalt A, Carlson EJ, Epstein CJ, Reeves RH. Craniofacial phenotypes in segmentally trisomic mouse models for Down syndrome. *Am J Med Genet.* 2002;107:317–324.

34. Seregaza Z, Roubertoux PL, Jamon M, Soumireu-Mourat B. Mouse models of cognitive disorders in trisomy 21: a review. *Behav Genet.* 2006;36:387–404..
35. Gardiner K, Fortna A, Bechtel L, Davisson MT. Mouse models of Down syndrome: how useful can they be?—comparison of the gene content of human chromosome 21 with orthologous mouse genomic regions. *Gene.* 2003;318:137–147.
36. Gardiner K, Costa AC. The proteins of human chromosome 21. *Am J Med Genet C Semin Med Genet.* 2006;142:196–205.
37. Ridder WH 3rd, Nusinowitz S. The visual evoked potential in the mouse: origins and response characteristics. *Vision Res.* 2006;46: 902–913.
38. Ren JC, LaVail MM, Peachey NS. Retinal degeneration in the nervous mutant mouse. III. Electrophysiological studies of the visual pathway. *Exp Eye Res.* 2000;70:467–473.
39. Chow E, Mottahedeh J, Prins M, Ridder W, Nusinowitz S, Bronstein JM. Disrupted compaction of CNS myelin in an OSP/claudin-11 and PLP/DM20 double knockout mouse. *Mol Cell Neurosci.* 2005;29: 405–413.
40. Tebano MT, Luzi M, Palazzesi S, Pomponi M, Loizzo A. Effects of cholinergic drugs on neocortical EEG and flash-visual evoked potentials in the mouse. *Neuropsychobiology.* 1999;40:47–56.
41. Henry KR, Rhoades RW. Relation of albinism and drugs to the visual evoked potential of the mouse. *J Comp Physiol Psychol.* 1978;92:271–279.
42. Porciatti V, Pizzorusso T, Maffei L. The visual physiology of the wild type mouse determined with pattern VEPs. *Vision Res.* 1999; 39:3071–3081.
43. Nusinowitz S, Ridder WH 3rd, Pang JJ, et al. Cortical visual function in the rd12 mouse model of Leber Congenital Amaurosis (LCA) after gene replacement therapy to restore retinal function. *Vision Res.* 2006;46:3926–3934.
44. Nusinowitz S, Ridder WH 3rd, Ramirez J. Temporal response properties of the primary and secondary rod-signaling pathways in normal and Gnat2 mutant mice. *Exp Eye Res.* 2007;84:1104–1114.
45. Davisson MT, Costa ACS. Mouse models of Down syndrome. *Adv Neurochem.* 1999;9:297–327.
46. Ridder W 3rd, Nusinowitz S, Heckenlively JR. Causes of cataract development in anesthetized mice. *Exp Eye Res.* 2002;75:365–370.
47. Campbell FW, Maffei L. Electrophysiological evidence for the existence of orientation and size detectors in the human visual system. *J Physiol.* 1970;207:635–652.
48. Pizzorusso T, Fagiolini M, Porciatti V, Maffei L. Temporal aspects of contrast visual evoked potentials in the pigmented rat: effect of dark rearing. *Vision Res.* 1997;37:389–395.
49. Mezer E, Bahir Y, Leibu R, Perlman I. Effect of defocusing and of distracted attention upon recordings of the visual evoked potential. *Doc Ophthalmol.* 2004;109:229–238.
50. Martin M, Hiltner TD, Wood JC, Fraser SE, Jacobs RE, Readhead C. Myelin deficiencies visualized in vivo: visually evoked potentials and T2-weighted magnetic resonance images of shiverer mutant and wild-type mice. *J Neurosci Res.* 2006;84:1716–1726.
51. Niklas A, Sebraoui H, Hess E, Wagner A, Then Bergh F. Outcome measures for trials of remyelinating agents in multiple sclerosis: retrospective longitudinal analysis of visual evoked potential latency. *Mult Scler.* 2009;15:68–74.
52. Martin M, Reyes SD, Hiltner TD, et al. T(2)-weighted microMRI and evoked potential of the visual system measurements during the development of hypomyelinated transgenic mice. *Neurochem Res.* 2007;32:159–165.
53. Siu TL, Morley JW. Suppression of visual cortical evoked responses following deprivation of pattern vision in adult mice. *Eur J Neurosci.* 2008;28:484–490.
54. Jackson GR, Owsley C. Visual dysfunction, neurodegenerative diseases, and aging. *Neurol Clin.* 2003;21:709–728.
55. Cosi V, Vitelli E, Gozzoli L, Corona A, Ceroni M, Callieco R. Visual evoked potentials in aging of the brain. *Adv Neurol.* 1982;32:109–115.
56. Partanen J, Hartikainen P, Kononen M, Jousmaki V, Soininen H, Riekkinen P Sr. Prolonged latencies of pattern reversal visual evoked early potentials in Alzheimer disease. *Alzheimer Dis Assoc Disord.* 1994;8:250–258.
57. Escorihuela RM, Fernandez-Teruel A, Vallina IF, et al. A behavioral assessment of Ts65Dn mice: a putative Down syndrome model. *Neurosci Lett.* 1995;199:143–146.
58. Seo H, Isacson O. Abnormal APP, cholinergic and cognitive function in Ts65Dn Down's model mice. *Exp Neurol.* 2005;193:469–480.
59. Stasko MR, Costa AC. Experimental parameters affecting the Morris water maze performance of a mouse model of Down syndrome. *Behav Brain Res.* 2004;154:1–17.
60. Moran TH, Capone GT, Knipp S, Davisson MT, Reeves RH, Gearhart JD. The effects of piracetam on cognitive performance in a mouse model of Down's syndrome. *Physiol Behav.* 2002;77:403–409.
61. Martinez-Cue C, Baamonde C, Lumbreras M, et al. Differential effects of environmental enrichment on behavior and learning of male and female Ts65Dn mice, a model for Down syndrome. *Behav Brain Res.* 2002;134:185–200.
62. Morris RG, Garrud P, Rawlins JN, O'Keefe J. Place navigation impaired in rats with hippocampal lesions. *Nature.* 1982;297:681–683.
63. Logue SF, Paylor R, Wehner JM. Hippocampal lesions cause learning deficits in inbred mice in the Morris water maze and conditioned-fear task. *Behav Neurosci.* 1997;111:104–113.
64. Robinson L, Bridge H, Riedel G. Visual discrimination learning in the water maze: a novel test for visual acuity. *Behav Brain Res.* 2001;119:77–84.